

Alveolar Macrophage Phenotype and Compartmentalization Drive Different Pulmonary Changes in Mouse Strains Exposed to Cigarette Smoke

Giovanna De Cunto, Eleonora Cavarra, Barbara Bartalesi, Giuseppe Lungarella & Monica Lucattelli

To cite this article: Giovanna De Cunto, Eleonora Cavarra, Barbara Bartalesi, Giuseppe Lungarella & Monica Lucattelli (2020): Alveolar Macrophage Phenotype and Compartmentalization Drive Different Pulmonary Changes in Mouse Strains Exposed to Cigarette Smoke, COPD: Journal of Chronic Obstructive Pulmonary Disease, DOI: [10.1080/15412555.2020.1783648](https://doi.org/10.1080/15412555.2020.1783648)

To link to this article: <https://doi.org/10.1080/15412555.2020.1783648>



© 2020 The Author(s). Published with license by Taylor & Francis Group, LLC



Published online: 29 Jun 2020.



Submit your article to this journal [↗](#)








View related articles [↗](#)



View Crossmark data [↗](#)

Alveolar Macrophage Phenotype and Compartmentalization Drive Different Pulmonary Changes in Mouse Strains Exposed to Cigarette Smoke

Giovanna De Cunto , Eleonora Cavarra , Barbara Bartalesi , Giuseppe Lungarella* , and Monica Lucattelli* 

Department of Molecular and Developmental Medicine, University of Siena, Siena, Italy

ABSTRACT

COPD can manifest itself with different clinical phenotypes characterized by different disease progression and response to therapy. Although a remarkable number of studies have been carried out, little is known about the mechanisms underlying phenotypes that could guide the development of viable future therapies. Several murine strains mirror some human phenotypes after smoke exposure. It was of interest to investigate in these strains whether different pattern of activation of macrophages, and their distribution in lungs, is associated to changes characterizing different phenotypes. We chose C57Bl/6, and Lck deficient mice, which show significant emphysema, DBA/2 mice that develop changes similar to those of “pulmonary fibrosis/emphysema syndrome”, *p66Shc* ko mice that develop bronchiolitis with fibrosis but not emphysema, and finally ICR mice that do not develop changes at 7 months after smoke exposure. Unlike other strains, ICR mice show very few activated macrophages (Mac-3 positive) mostly negative to M1 or M2 markers. On the other hand, a large population of M1 macrophages predominates in the lung periphery of DBA/2, C57Bl/6 and in Lck deficient mice, where emphysema is more evident. M2 macrophages are mainly observed in subpleural and intraparenchymal areas of DBA/2 mice and around bronchioles of *p66Shc* ko mice where fibrotic changes are present. We observed slight but significant differences in mRNA expression of iNOS, ECF-L, arginase 1, IL-4, IL-13 and TGF- β between air- and smoke-exposed mice. These differences together with the different compartmentalization of macrophages may offer an explanation for the diversity of lesions and their distribution that we observed among the strains.

ARTICLE HISTORY

Received 14 May 2020
Accepted 11 June 2020

KEYWORDS

Mouse strain differences; smoking exposure; alveolar macrophage activation; emphysema; bronchiolar remodeling; COPD phenotypes

Introduction



Clinically, chronic obstructive pulmonary disease (COPD) presents as one of several different phenotypes with different prognosis [1,2].

Risk factors for developing this pulmonary disease include genetic abnormalities that increase susceptibility, such as alpha-1-proteinase inhibitor (alpha1 PI) deficiency, cigarette smoking and exposure to several environmental factors, such as air pollutants [3]. Although, in the last two decades, a remarkable number of scientific studies have been carried out on COPD, many facets of its pathogenesis are not fully understood.

In this context, animal models of COPD involving cigarette smoking have proven to be of central importance to clarify the role of individual responses and the genetic basis of the different sensitivity to develop the disease [4,5]. Therefore, as in humans, some mouse strains (such as C57 Bl/6 and DBA/2) develop significant emphysema when exposed to cigarette smoke for 7 months, whereas other mice (such as ICR) do not [6]. Likewise, cigarette smoking

leads to various phenotypes of disease in the different mouse strains [7–11] which can also be found in human patients.

Very recent studies conducted in both humans and animals indicate that innate inflammatory cells activated by different stimuli on the cell surface are needed to develop pulmonary changes caused by cigarette smoking [12–21]. Smoking exposure induces proinflammatory response through the activation of pattern recognition receptors (PRRs) by damage-associated molecular patterns (DAMPs) release (i.e. AGE, endogenous ATP, formylpeptides, HMGB1, MyD88 etc.) [13–17,20,22–24]. This results in innate immune responses and in the release of IL-1 β , MCP-1 as well as MIP-2 and KC, the mouse homolog for human IL-8, which regulate migration and infiltration of neutrophils and monocytes/macrophages. These cells promote an overload of oxidants and proteases that lead to epithelial damage and cell death. Neutrophils and macrophages were initially involved in tissue injury and lung dysfunction, however, some proteases released from these cells can perform many regulatory functions through the activation of chemokines and cytokines, the

CONTACT Giuseppe Lungarella  giuseppe.lungarella@unisi.it  Department of Molecular and Developmental Medicine, University of Siena, via aldo Moro n. 2, Siena I-53100, Italy.

*Equally contributed to this work.

© 2020 The Author(s). Published with license by Taylor & Francis Group, LLC

This is an Open Access article distributed under the terms of the Creative Commons Attribution-NonCommercial-NoDerivatives License (<http://creativecommons.org/licenses/by-nc-nd/4.0/>), which permits non-commercial re-use, distribution, and reproduction in any medium, provided the original work is properly cited, and is not altered, transformed, or built upon in any way.

shedding or even activation of receptors of the cell surface, called proteinase-activated receptors (PARs) [25].

Several studies in animals and man suggest that alveolar macrophages play a central role in the pathophysiology of COPD and may orchestrate the chronic inflammatory responses [26]. The natural plasticity of macrophages can give rise to different cell populations, changed in phenotype and function, capable of greatly influencing the inflammatory or reparative response, and therefore the phenotype of the disease.

In fact, several cell populations have been described in COPD, resulting from resident macrophages or from blood monocytes, which once activated can exhibit at least two main different polarized phenotypes called M1 (pro-inflammatory) and M2 (reparative) subpopulations.

What we do not know at the moment is:

- the compartmentalization of macrophage subpopulations in lung structures during the destructive and remodeling processes that characterize COPD, and
- whether the presence of different activated macrophage subpopulations is really associated with different anatomical changes.

These factors could contribute to the development of the different phenotypes of the disease.

The availability in our laboratory of different mouse strains, which in some respects reflect the phenotypes of human COPD after chronic cigarette smoke exposure [6–11,24], represented an inviting opportunity for us to study macrophage activation, polarization and their distribution in the lung tissue in the different murine phenotypes. Therefore, the main purpose of this work was to study selected mouse strains if the different activation pattern of macrophages and their distribution in the lungs is associated with cigarette smoke-induced changes that characterize different disease phenotypes.

Materials & methods

Animal experiments

Male mice from different strains (4–6 wk old) were used in this study. C57 Bl/6, DBA/2 and ICR were supplied from Charles River (Calco, Italy). Dr. P.G. Pellicci at the European Institute of Oncology, Milan, kindly provided 129 *p66^{Shc}* knockout breeding pairs. The breeding stocks were backcrossed onto 129/SVEv mice (supplied by Charles River Italia, Calco, Italy) to full congenic status and a colony of these mice is maintained in our animal facility. Lck-deficient (*Lck^{-/-}*) mice with C57 Bl/6 background were initially obtained from The Jackson Laboratory (Bar Harbor, ME). The colonies were expanded at Charles River' husbandries (Calco, Italy) and then supplied to Siena University animal house.

The mice were housed in an environment controlled for light (7 AM to 7 PM) and temperature (18 °C to 22 °C); food (Mucedola Global Diet 2018; Harlan, Corezzana, Italy) and water were provided for consumption *ad libitum*. All animal experiments were conducted in conformity with the "Guiding Principles for Research Involving Animals and

human Beings" and were approved by the Local Ethics Committee of the University of Siena.

Exposure to cigarette smoke

Mice from each strain were exposed to either room air (controls) or to the smoke of three cigarettes/day, 5 days/week for 5 or 7 months, (Virginia filter cigarettes, 12 mg of tar and 0.9 mg of nicotine) (smoking group). The methodology for smoke exposure has previously been described in detail [6].

At the various time intervals during the chronic exposure to cigarette, six animals from smoke or room air groups and from each strain were anesthetized with sodium pentobarbital, sacrificed by severing the abdominal aorta and the lungs were immediately removed.

Morphology and morphometry

Lungs were fixed intra-tracheally with formalin (5%) at a pressure of 20 cm H₂O. Post-fixation lung volume was measured by water displacement. Lungs were processed for histology and stained with haematoxylin–eosin, periodic acid-Schiff (PAS) or Masson's trichrome. Lung slides were analysed for morphology and morphometry. Assessment of emphysema included mean linear intercept (Lm) and internal surface area (ISA) [27–29]. Lm represents the average size of air space (alveolar ducts, alveolar sacs and alveoli). Lm is the length of a test line placed over histologic slides of the lung, divided by the number of times the line crosses alveolar walls (not surfaces). The determination of the Lm was carried out by two blinded pathologists. Fields with bronchi, large bronchioles, or blood vessels were excluded from the measurements. Lm values were used to calculate the ISA, necessary for evaluating the degree of emphysema, from the equation $4V/Lm$, where V is the post-fixation lung volume [28,29]. For the determination of the Lm for each pair of lungs, 40 histologic fields were evaluated both vertically and horizontally. Examination of this many fields meant that practically the entire lung area was evaluated [14]. Fibrosis was evidenced in tissue slides after Masson's trichrome staining and the extent of fibrosis was carried out on randomly sampled areas of lungs [30,31]. Morphometric assessment consisted of the determination by point counting of the percent volume density of fibrosis $Vv(f)$ according to the stereological principle of Glagoleff and Weibel [32]: $Vv = Pp$, where Vv is the volume density and Pp is the fraction of points superimposed the structural change. Point counting was performed at 200× by determining 20 random fields per slide and using a multipurpose grid to count 48 points per field for a total of 960 points per slide.

Inflammatory cells profile in BALF

The total and differential cell counts in bronchoalveolar lavage fluids (BALFs) were carried out in mice from each group at 5 months from the start of the study. Before removing lungs, the tracheas were isolated *in situ* in animals under anaesthesia and then cannulated with a 20-gauge blunt needle. With the aid of a peristaltic pump (P-1

Table 1. Primers and probes used for real-time RT-PCR.

Gene	Primers	Amplicon's length	UPL probe
<i>Tgfb1</i>	Fw 5' TGG AGC AAC ATG TGG AAC TC-3'/Rev 5' GTC AGC AGC CGG TTA CCA-3'	73 nt	#42
<i>il4</i>	Fw 5' CAT CGG CAT TTT GAA CGA G 3'/Rev 5'CGA GCT CAC TCT CTG TGG GTG 3'	104 nt	#2
<i>il13</i>	Fw 5' CCT CTG ACC CTT AAG GAG CTTAT3'/Rev 5' CGT TGC ACA GGG GAG TCT 3'	70 nt	#17
<i>ecfl</i>	Fw 5'AAG AAC ACT GAG CTA AAA ACT CTC CT 3'/Rev 5' GAG ACC ATG GCA CTG AAC G 3'	77 nt	#88
<i>Arg1</i>	Fw 5' GAA TCT GCA TGG GCA ACC 3'/Rev 5' GAA TCC TGG TAC ATC TGG GAA C 3'	73 nt	#2
<i>Nos2</i>	Fw 5' CTT TGC CAC GGA CGA GAC 3'/Rev 5' TCA TTG TAC TCT GAG GGC TGA C 3'	76 nt	#13

Pharmacia), the lungs were lavaged *in situ* three times with 0.6 ml saline solution. The average fluid recovery was greater than 95%. The number of neutrophils, macrophages and lymphocytes was assessed by using Diff-Quick staining.

Immunohistochemistry

Tissue sections (5 μ m thick) were stained for inducible nitric oxide synthase (iNOS), chitinase-like 3 (ECF-L), arginase 1 using the immunoperoxidase method. MAC-3 was stained using the streptavidin-HRP method. The primary antibodies (Ab) used were rat monoclonal Ab to mouse Mac-3 (1:20, BD Pharmingen, Buccinasco, Italy); rabbit polyclonal Ab to mouse iNOS (1:100, Abcam Ltd, Cambridge, UK); goat polyclonal Ab to mouse ECF-L (1:250, R&D Systems Europe, LTD, Abingdon, UK); mouse monoclonal Ab to arginase I (1:100, BD Pharmingen, Buccinasco, Italy). All sections were rinsed and incubated for 30 min at room temperature with biotinylated mouse anti-rat IgG diluted 1:100 (Abcam, Cambridge, UK) to detect Mac-3; with sheep anti-rabbit IgG diluted 1:200 (Sigma) to detect the expression of iNOS; with rabbit anti-goat IgG diluted 1:200 (Sigma) to detect ECF-L.

To localize mouse primary monoclonal antibodies to arginase I on mouse tissues, we used the Vector M.O.M. immunodetection kit (Vector Laboratories, Burlingame, CA, USA) containing a novel blocking agent designed specifically to reduce the undesired background staining. Immunostaining was revealed by using the M.O.M. detection kit with 3,3'-diaminobenzidine tetra hydrochloride (DAB) substrate. As negative controls for the immunostaining, the primary Ab was replaced by non-immunized serum.

RNA isolation and cDNA synthesis

Total RNA was extracted from the lungs of mice by using Tri Reagent (Ambion, Austin, TX) according to the manufacturer's instructions. Five mice for each group were used for RNA isolation. RNA was re-suspended in RT-PCR Grade Water (Ambion), and the amount and purity of RNA were quantified spectrophotometrically by measuring the optical density at 260 and 280 nm. Integrity was checked by agarose gel electrophoresis. Two micrograms of total RNA were treated with TURBO DNase (TURBO DNA-free kit; Ambion) for 30 min and reverse transcribed by using the RETROscript kit (Ambion), according to the manufacturer's instructions. Two hundredths of the final volume of RT were used for real-time RT-PCR.

Table 2. Effect of chronic exposure to cigarette smoke on lung morphometry in various strains of mice at 7 months from the start of the exposure treatment.

Strain	Exposure	Lm (μ m)	ISA (cm ²)	VL (ml)
ICR	Air	40.75 \pm 0.73	1 180 \pm 68	1.20 \pm 0.07
ICR	Cigarette smoke	42.61 \pm 0.81	1 169 \pm 71	1.24 \pm 0.08
C57 Bl/6	Air	41.52 \pm 0.63	1 203 \pm 65	1.25 \pm 0.08
C57 Bl/6	Cigarette smoke	48.05 \pm 1.30*	1 021 \pm 60*	1.23 \pm 0.08
DBA/2	Air	38.51 \pm 0.90	1 257 \pm 54	1.21 \pm 0.06
DBA/2	Cigarette smoke	49.15 \pm 1.25*	1 073 \pm 64*	1.32 \pm 0.15
C57 Bl/6 ^{Lck-/-}	Air	40.59 \pm 0.69	1 182 \pm 61	1.20 \pm 0.08
C57 Bl/6 ^{Lck-/-}	Cigarette smoke	50.87 \pm 1.75*	924 \pm 52*	1.18 \pm 0.09
129/SVEv ^{p66Sh-/-}	Air	39.97 \pm 0.60	1 189 \pm 50	1.18 \pm 0.08
129/SVEv ^{p66Sh-/-}	Cigarette smoke	41.02 \pm 0.62	1 178 \pm 55	1.21 \pm 0.08

Data are presented as mean \pm SD. Six animals for each group were used.

* $p < 0.01$ vs air control mice of the same strain.

ISA: internal surface area of lungs; Lm: mean linear intercepts; VL: post fixation lung volume.

Real-time RT-PCR

Real-time RT-PCR was performed in triplicate for each sample on the MJ Opticon Monitor 2 (MJ Research Co., Waltham, MA) with specific locked nucleic acid probes from the Mouse Universal Probe Library Set (Roche, Indianapolis, IN). Primers were designed by using the free online ProbeFinder software version 2.53 (Roche Molecular Systems Inc., Branchburg, NJ) that shows a pair of specific primers for each probe from the Universal Probe Library set (Roche) (Table 1). The combination of primers and probes provides specific amplification and detection of the target sequence in the sample. PCR reactions were performed in a volume of 25 μ L containing 12.5 μ L of FastStart TaqMan Probe Master(Roche), 300 nmol/L forward and reverse primers (TIBMolbiol, Genova, Italy), 200 nmol/L Universal Probe Library Set probes and 5 μ L of cDNA. The real-time RT-PCR assay was performed according to a method reported in detail in our previous studies [11,24].

The average of the target gene was normalized to 18S rRNA as the endogenous housekeeping gene [33].

Statistical analysis

Data are presented as mean \pm SD. The significance of the differences was calculated using one-way analysis of variance (*F*-test). A *p* value < 0.05 was considered significant.

Results

Morphology and morphometry

As previously reported in our studies, two major types of lesions affecting lung parenchyma at various degrees can be seen at 7 months in the cigarette smoking mice, namely emphysema and fibrosis. However, there are clear

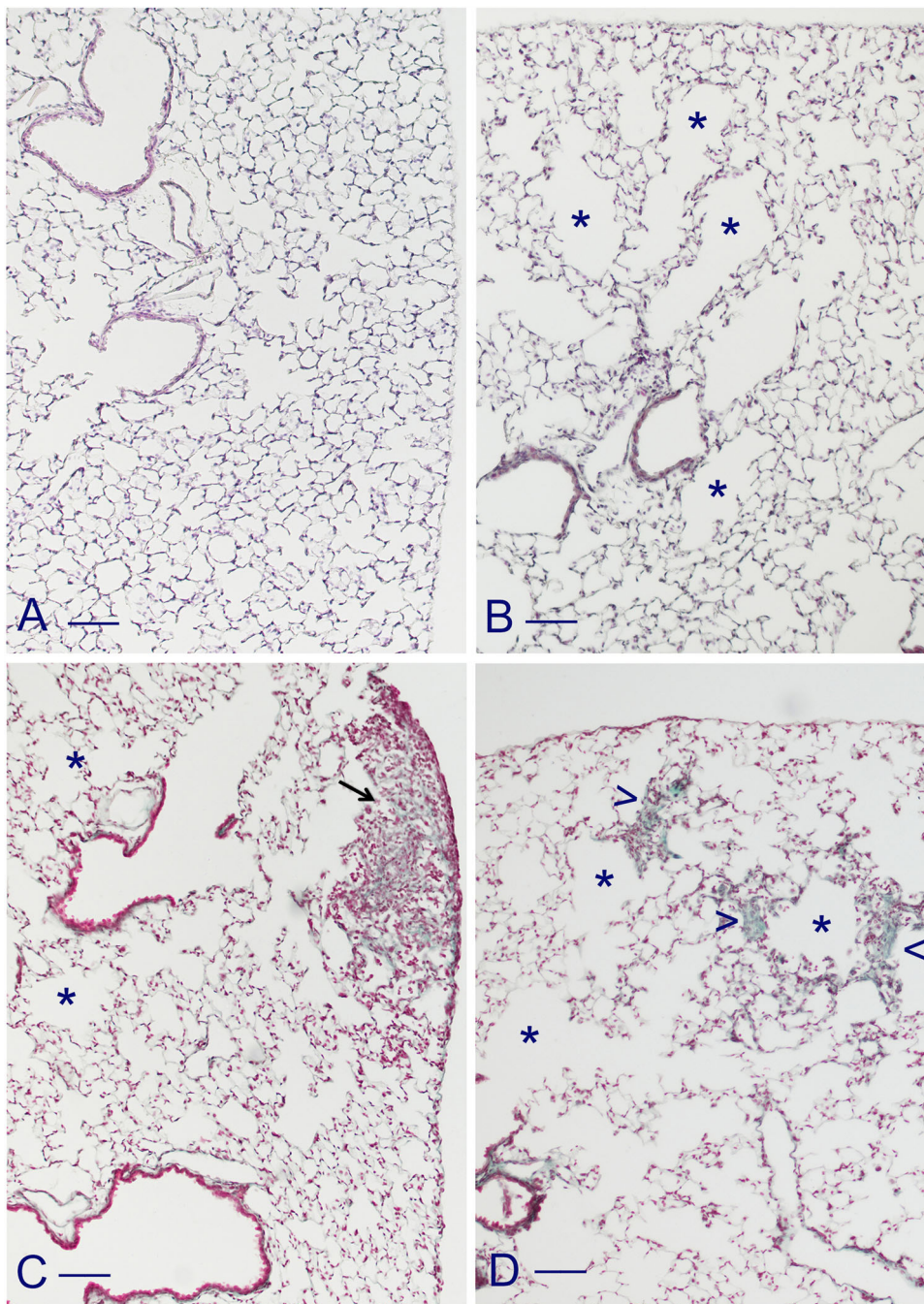


Figure 1. Photomicrographs of lung sections stained with Masson's trichrome from smoking ICR, C57 Bl/6 and DBA/2 mice at 7 months from the start of experiments. ICR mice display a well-fixed parenchyma with a normal architecture (A). C57 Bl/6 mice show multiple areas of emphysema (*) scattered throughout the parenchyma (B). In DBA/2 mice emphysematous changes (*) are present together with evident fibrotic lesions located mainly in subpleural areas (C, arrow) and some intraparenchymal fibroproliferative changes characterized by infiltration of inflammatory cells and deposition of extracellular matrix ("sea green areas") (D, arrowheads). Scale bars = 100 μ m.

differences in the morphology of these pathologies among the mice chosen for such a study.

The quantification of emphysema in the different strains carried out at 7 months after CS-exposure included determination of the average inter-alveolar distance (mean linear intercept: Lm) and internal surface area (ISA) estimated by the Lm method at post-fixation lung volume. The post-fixation lung volumes as well as Lm and of ISA values obtained in all the strains after 7 months exposure either to room air or to cigarette smoke are presented in Table 2. No difference

between post fixation lung volumes from air control and smoking animals of the same strain is observed.

As can be seen, neither the ICR mice nor *p66* knockout mice have Lm and ISA mean values different from those of the respective controls. On the other hand, emphysema is observed in C57 Bl/6, DBA/2 and *Lck* knockout mice in which Lm and ISA values significantly differ from those of air-exposed groups (Table 2).

At 7 months after CS-exposure, the lungs of ICR mice show some foci of mild intra-alveolar, peri-bronchial or peri-

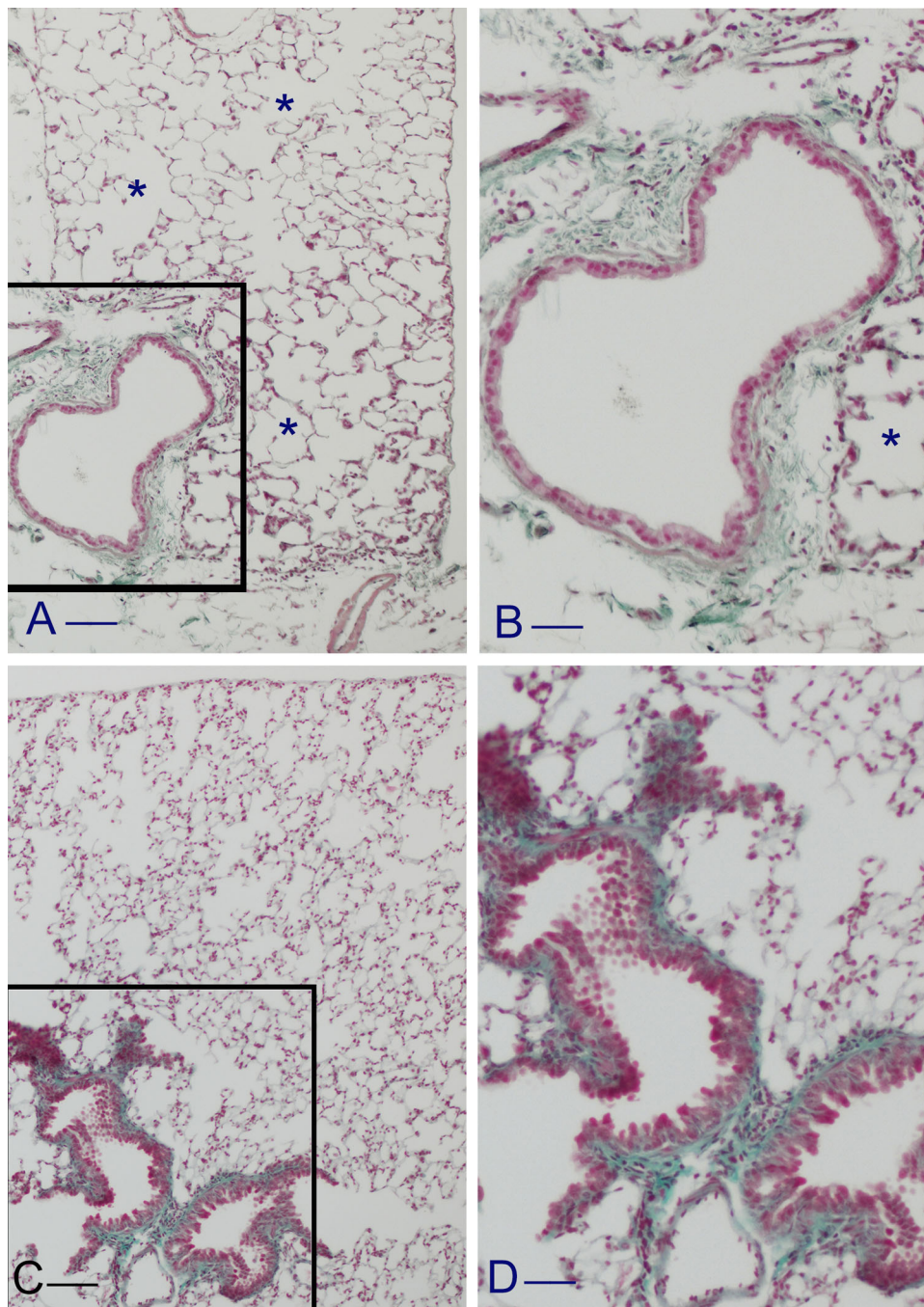


Figure 2. Representative lung parenchyma from *Lck* and *p66Shc* knockout mice after Masson's trichrome stain. At 7 months after cigarette smoke exposure, lung parenchyma from *Lck* deficient mice show patchy areas of emphysema (*) throughout the parenchyma (A) and a mild deposition of extracellular matrix in peribronchiolar areas (A). (B) is higher magnification of (A) showing a peribronchiolar area with slight increase of collagen deposition ("sea green area"). At 7 months from the start of the treatment smoking *p66Shc* deficient mice show significant collagen deposition ("sea green areas") in the peribronchiolar spaces throughout the lung parenchyma (C). These changes are not associated with significant areas of emphysema. (D) is higher magnification of (C). Scale bars = (A and C) 100 μm ; (B and D) 50 μm .

vascular infiltration of mononuclear cells with modest participation of neutrophils. Otherwise the parenchyma and airways of smoking ICR mice appear normal (Figure 1(A)). Trivial patchy areas of air space enlargement are seen in lungs of *p66* deficient mice (Figure 2(C)). In contrast, C57 Bl/6 (Figure 1(B)), DBA/2 (Figure 1(C,D)) and *Lck* (Figure 2(A)) knockout mice show multiple areas of emphysema dispersed in the parenchyma. Lm and ISA values corroborate the morphology evaluation of emphysema in these mice (Table 2).

Air-exposed control mice from all the strains exposed to room air show a well-fixed normal parenchyma with normal airways (data not shown).

As for fibrosis, fibrotic areas have been observed in DBA/2 mice (Figure 1(C,D)) and *p66* deficient animals (Figure 2(C,D)), but the severity and distribution are different in these strains. In *p66* deficient mice, significant collagen deposition ("sea green areas") is observed in the peribronchiolar spaces throughout the lung parenchyma (Figure

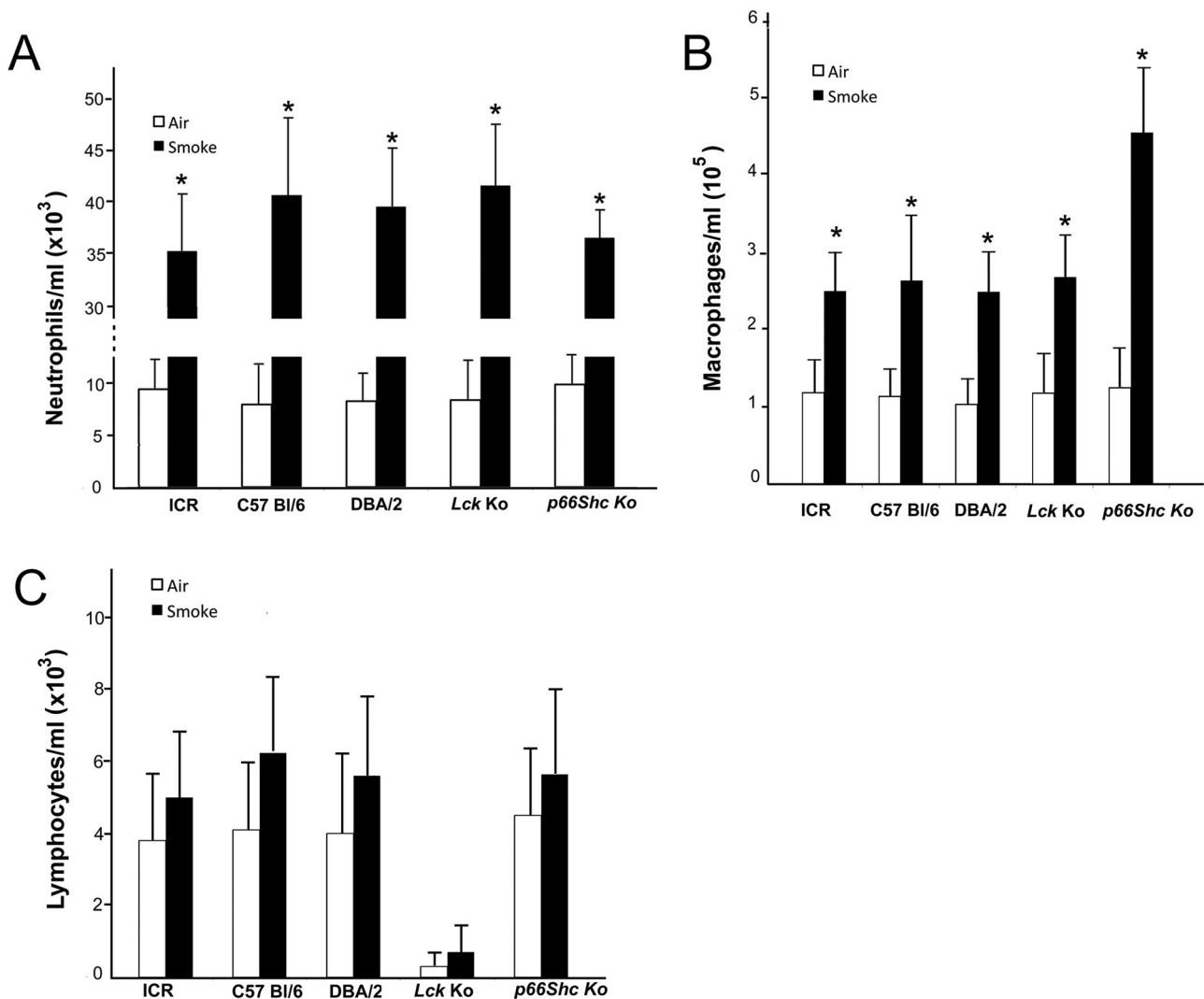


Figure 3. Inflammatory cells profile in BALFs from each strain and experimental group is reported in figure. No substantial difference in differential cell counts is found among strains of mice exposed to room air at 5 months from the start of the exposures (A, B and C), with the exception of *Lck* knockout mice that show a very low number of lymphocytes. After 5 months of smoke exposure, the number of neutrophils and macrophages in all the strains is significantly higher than that found in BALFs from their respective air exposed controls (A and B). On the contrary, no difference in lymphocyte counts is observed between smoking and air-exposed groups of the same strains (C). Data are expressed as means \pm SD from 6 mice per experimental group. They represent data from BALFs of mice exposed for 5 months to air or cigarette smoke. The slides were stained with Diff Quick. * $p < 0.05$ versus air exposure.

2(D)), while rare and small foci of fibroproliferative changes can be observed in the lung parenchyma. In these mice, fibrous changes are not associated with significant areas of emphysema (Figure 2(C)).

On the other hand, in mice belonging to the DBA/2 strain emphysematous alterations are present together with fibrotic lesions consisting mainly of subpleural foci (Figure 1(C)) and some parenchymal areas showing alveolar septa thickened by the infiltration of inflammatory cells and deposition of extracellular matrix (“sea green areas”) (Figure 1(D)). This picture is very similar to that described in human “pulmonary fibrosis/emphysema syndrome”.

At 7 months after exposure to CS, only a slight accumulation of collagen is observed in the peribronchiolar areas in C57 Bl/6 and *Lck* knockout mice with emphysema (Figure 2(B)).

The morphometric assessment of fibrosis was performed by point counting in DBA/2 and p66 deficient mice at 7 months after starting treatment. The volume density of fibrosis in

DBA/2 mice and p66 deficient animals was $6.3 \pm 1.4\%$ and $5.7 \pm 1.4\%$, respectively. Both these data are significantly different ($p < 0.01$) from those of the respective controls that have no fibrosis. Although the values we observed between the two strains after exposure to CS are very similar, the tissue distribution of the collagen accumulated in the lung is very different (Figures 1(C,D) and 2(C,D)).

Inflammatory cells profile in BALFs at 5 months from the start of the study

The total number of BAL cells $\times 10^5/\text{ml}$ in air control mice of the five strains is 1.53 ± 0.20 ; 1.58 ± 0.16 ; 1.49 ± 0.14 ; 1.46 ± 0.21 ; 1.63 ± 0.27 for ICR, F, DBA/2, *Lck* deficient and *p66^{Shc}* knockout mice, respectively.

The number of neutrophils, macrophages and lymphocytes in air-exposed mice from the different strain is reported in Figure 3(A, B and C), respectively. Of interest, no substantial

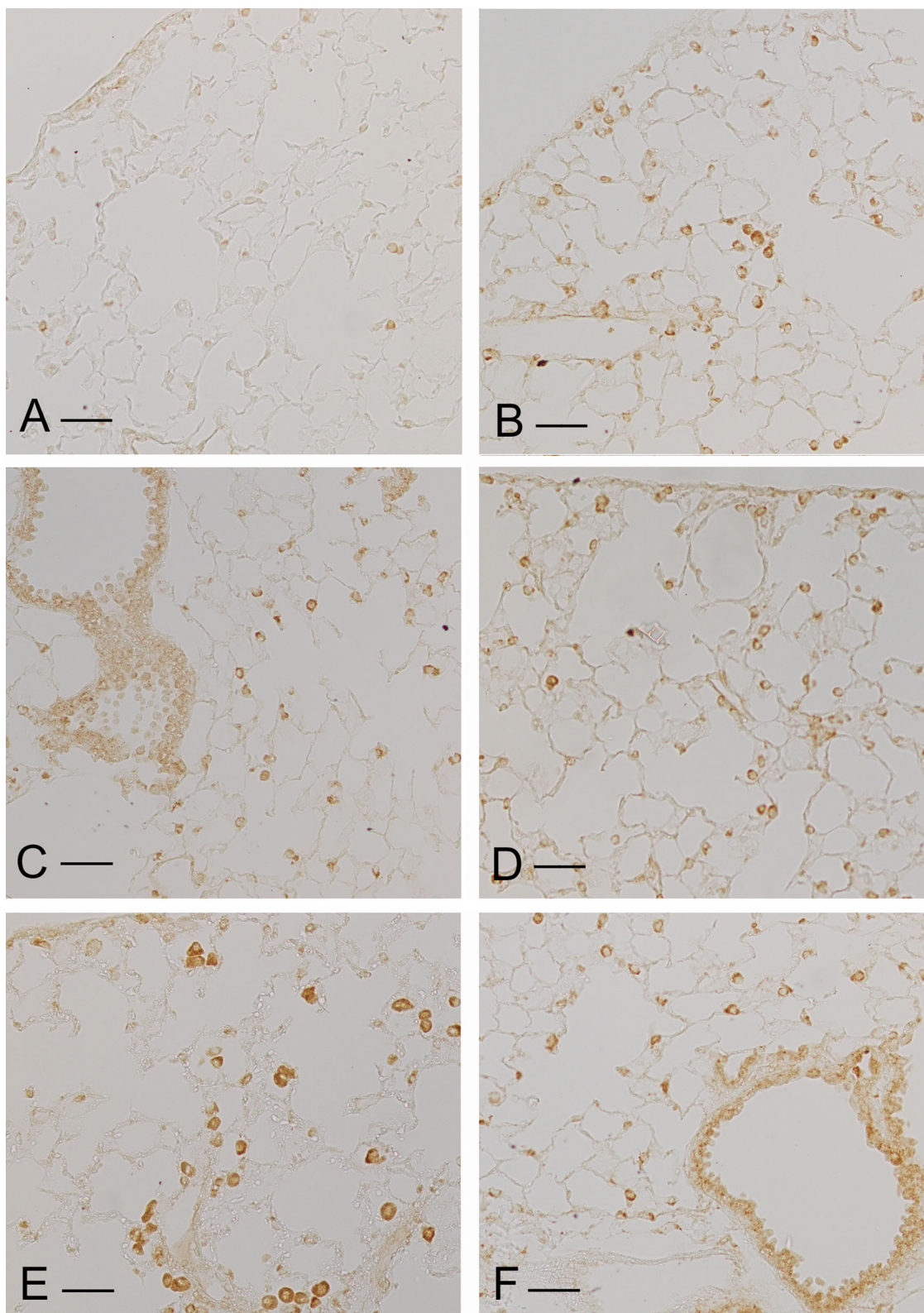


Figure 4. Immunohistochemical reaction for macrophage Mac-3 on lung parenchyma of ICR (A), C57 Bl/6 (B), DBA/2 (C), Lck deficient (D) and *p66Shc* ko (E, F) mouse. Mac-3 positive stained activated macrophages are seen throughout the lung parenchyma of C57 Bl/6, DBA/2, Lck deficient and *p66Shc* ko mice. Only few macrophages show this mark of activation in lungs of smoking resistant ICR mice. Scale bars = 50 μ m.

difference in total cell counts is found among strains of mice exposed to room air as well as to cigarette smoke.

In particular, as can be seen in [Figure 3\(A,B\)](#), no difference in term of neutrophils and macrophages is observed among air exposed ICR, C57 Bl/6, DBA/2, Lck deficient

mice and *p66* knockout animals at 5 months from the start of the exposure. In all the strains, the total number of neutrophils and macrophages in BALFs from smoking groups is significantly higher than that found in BALFs from air exposed mice.

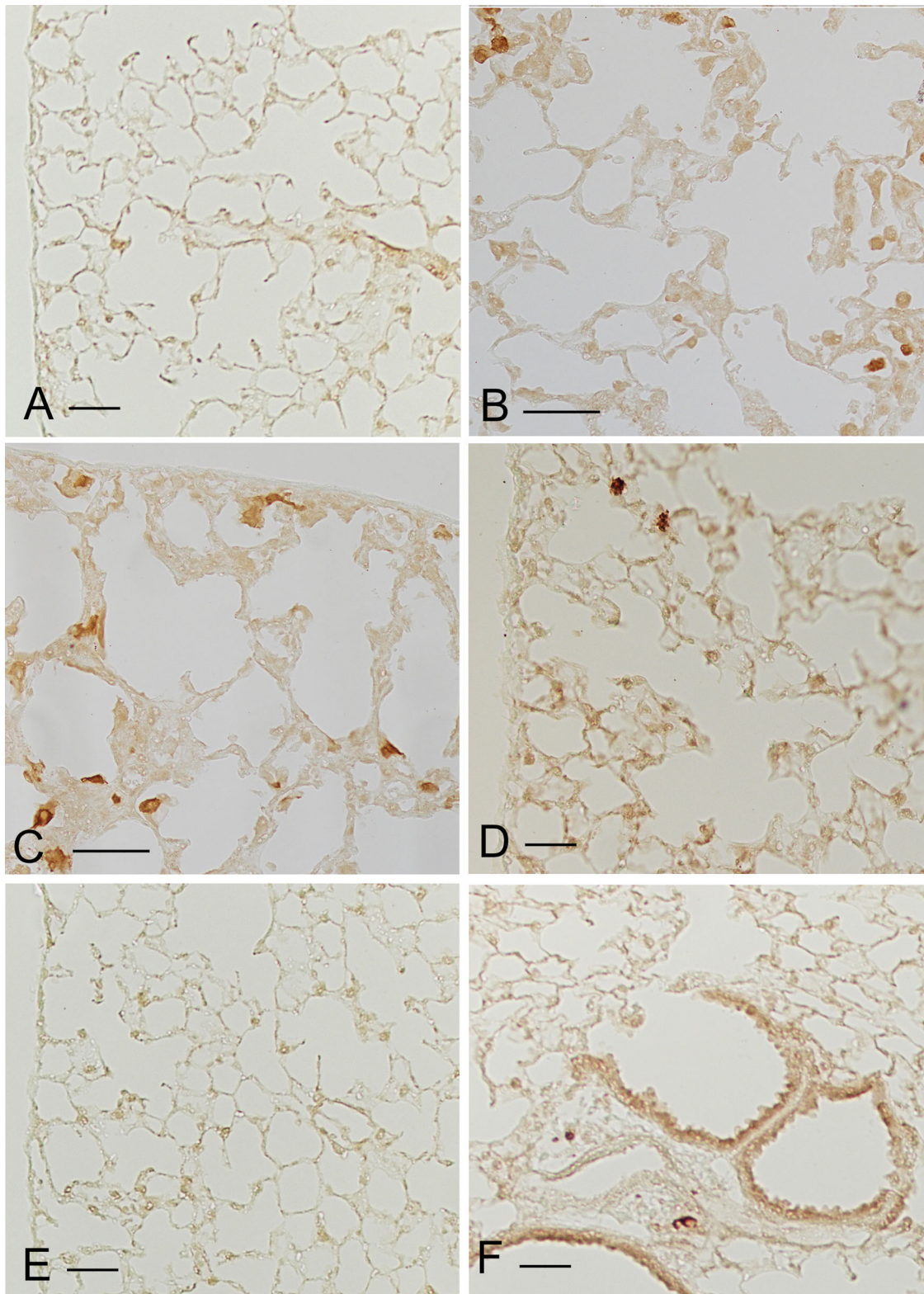


Figure 5. Immunohistochemical reaction for iNOS on lung slides obtained from smoke-exposed mice at 5 months from the start of experiments. A relevant number of iNOS positive macrophages (M1 type macrophages) is found in C57 Bl/6, DBA/2, and *Lck* knockout (B, C and D, respectively), in which moderate or severe areas of emphysema are present at 7 months of cigarette smoke exposure. Only a negligible number of iNOS positive macrophages is present in ICR mice, or in p66 knockout animals (A, E and F) that do not develop emphysema after chronic cigarette smoke exposure. Scale bars = 50 μ m.

The number of lymphocytes (Figure 3(C)) in BAL is practically the same in air exposed ICR, C57 Bl/6 and DBA/2 strains, as well as in p66Shc deficient animals, with the exception of *Lck* knockout mice that show an extremely low

number of lymphocytes both in the group exposed to air and to smoke. After smoke exposure, we do not see significant difference between smoking and air-exposed groups of the same strains (Figure 3(C)).

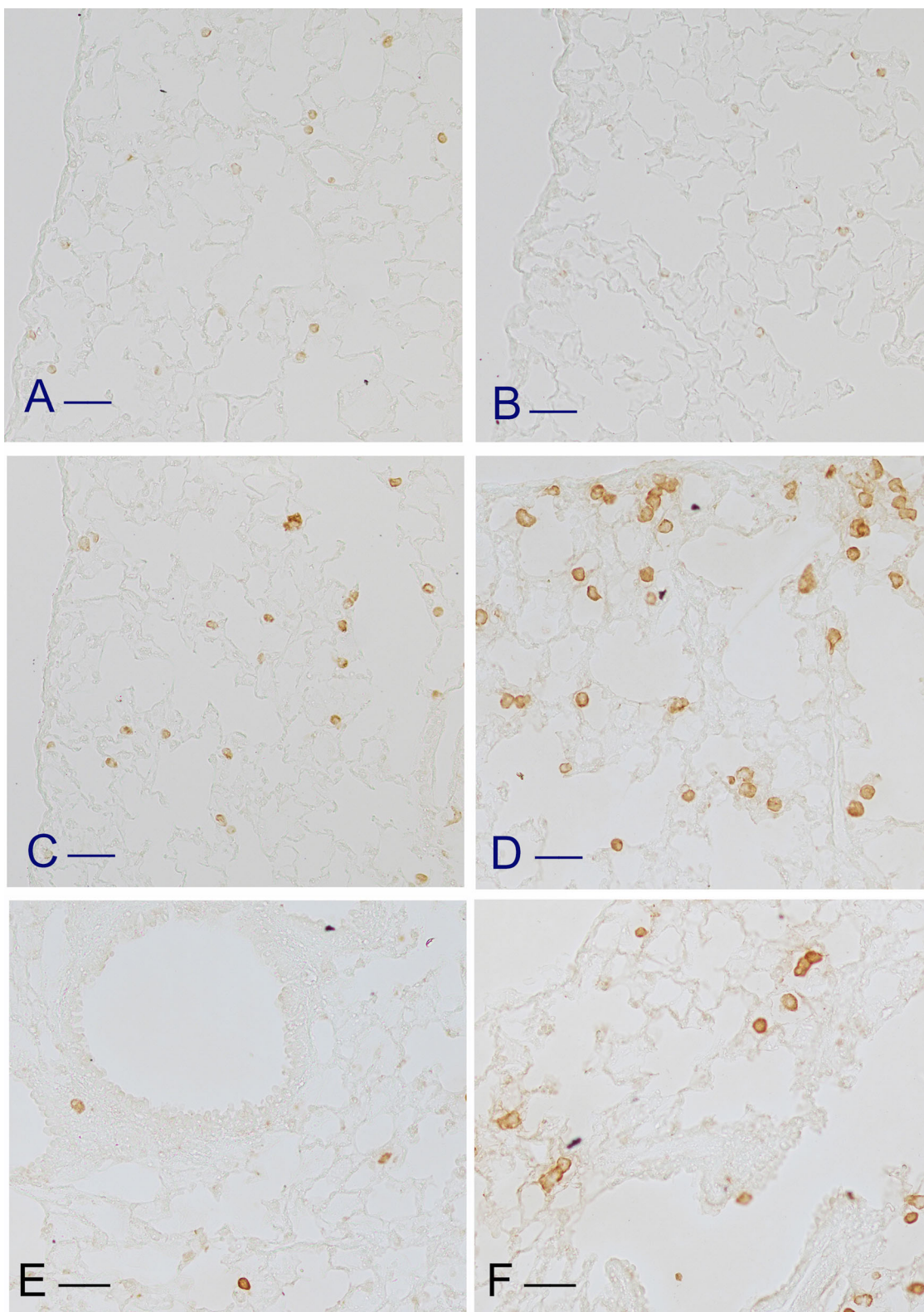


Figure 6. Immunohistochemical staining for chitinase-3like protein (ECF-L) in lungs of mice exposed to cigarette smoke for 5 months. A remarkable number of ECF-L positive macrophages are seen in lung parenchyma of mice that develop consistent fibrotic lesions such as DBA/2 (C and D) and p66 deficient mice (F). A trivial number of macrophages showing positivity for ECF-L is found in lung tissue of ICR (A), C57 Bl/6 (B) and *Lck* knockout mice (E). Scale bars = 100 μ m.

Activation, polarization and compartmentalization of lung macrophages of smoking mice

Micrographs of the immunohistochemistry for Mac3 in the lung of various mouse strains exposed to cigarette-smoke are

reported in Figure 4(A–F). As can be seen, a very few macrophages showing this mark of activation are found in lungs of smoking resistant ICR mice (Figure 4(A)). On the contrary, a large number of activated macrophages are appreciable in peripheral and in central areas of the lung parenchyma of the

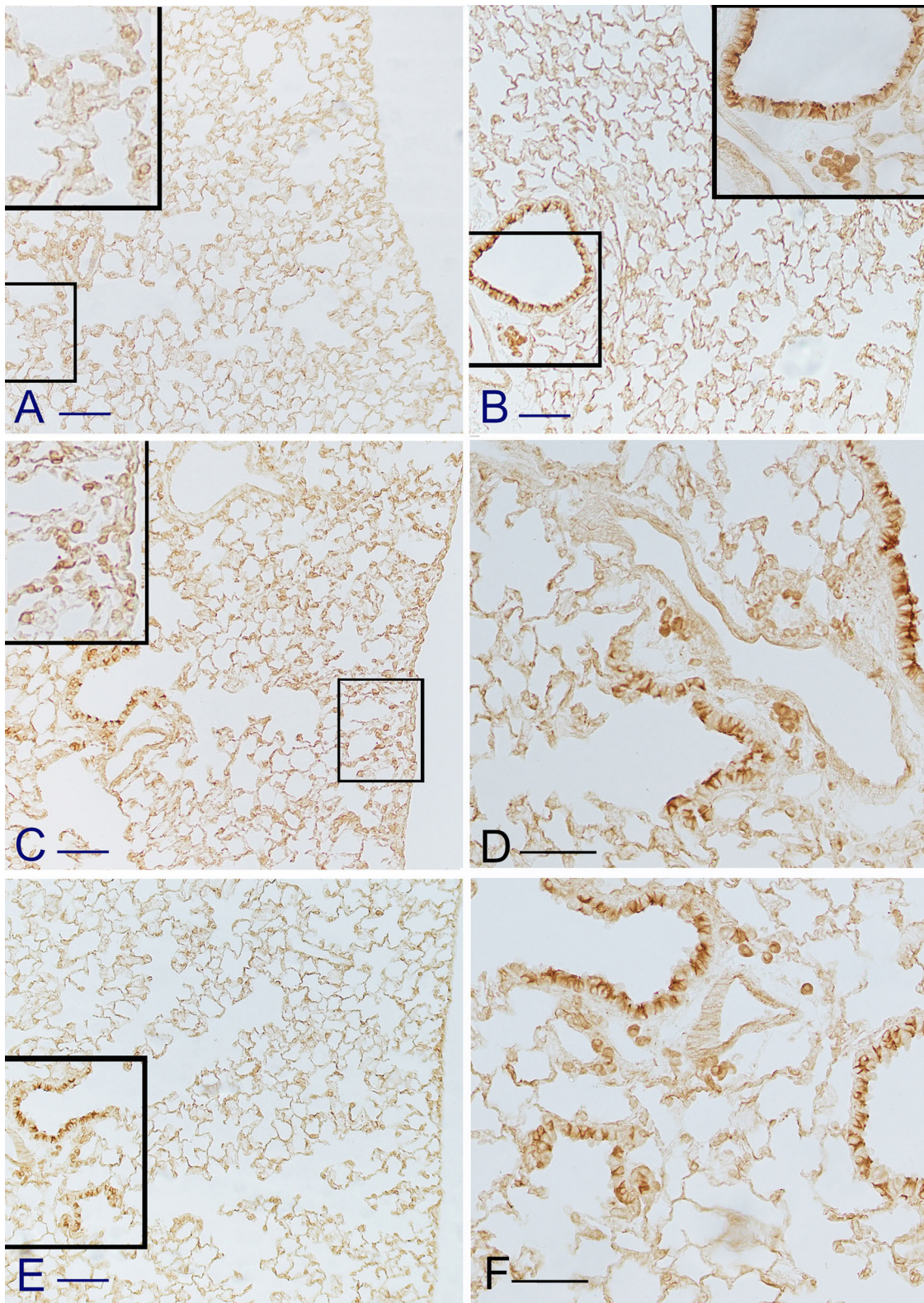


Figure 7. Immunohistochemical reaction for arginase 1 in smoking mice at 5 months from the start of the treatment. DBA/2 show a strong positivity for arginase 1 both in peripheral (C) and peribronchiolar areas (D) of their lungs. Similarly, in p66 deficient mice a consistent number of arginase 1 positive cell is found in peribronchiolar areas (E). (F) is higher magnification of (E). Few numbers of macrophages showing positivity for such an enzyme is found in C57 Bl/6J (B), or *Lck* deficient mice. No reaction is observed in macrophages from ICR mice (A). Scale bars: (A–C) = 100 μ m; (D–E) = 50 μ m.

other strains of mice at 5 months after CS exposure (Figure 4(B–F)). Positivity for Mac3 signal is generally not observed in lung macrophages from air-exposed controls (data not shown).

In mouse strains such C57 Bl/6, DBA/2 and *Lck* knock-out, where moderate or severe areas of emphysema are present after CS-exposure 7 months of treatment, a considerable number of iNOS positive macrophages (M1

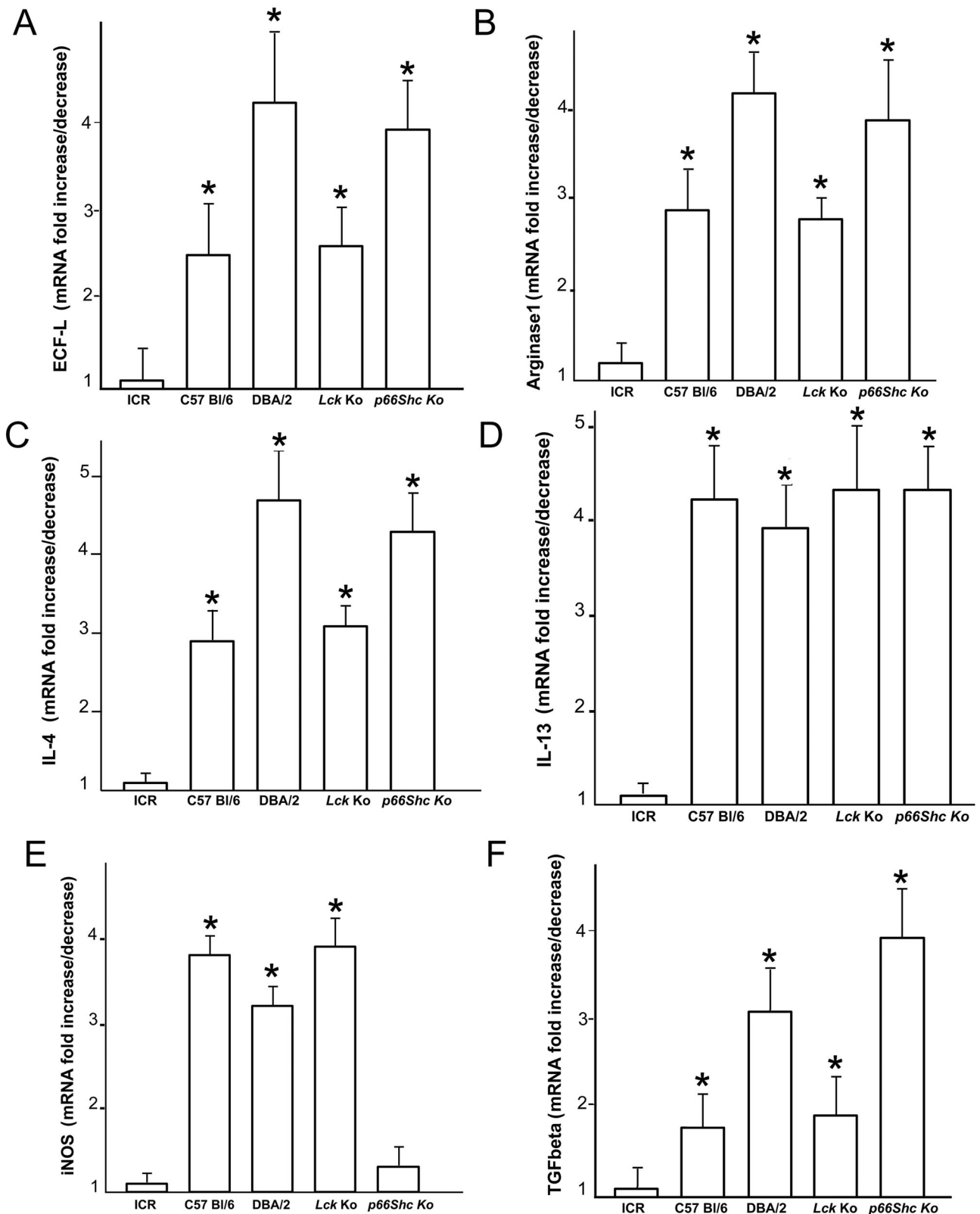


Figure 8. Real-time PCR analysis of mRNA for ECF-L (A), arginase 1 (B), IL-4 (C), IL-13 (D), iNOS (E) and TGF- β (F) carried out on lungs from six mice for each experimental group at 5 months after cigarette smoke exposure. Values are corrected for 18S rRNA and normalized to a median control value of 1.0. Data are presented as means \pm SD. * $p < 0.05$ versus air control values of the same genotype.

macrophages) is observed at 5 months especially in the peripheral areas of the lung (Figure 5(B–D)). In contrast, a negligible number of M1 macrophages are present in ICR mice, or in p66 knockout animals that do not

develop emphysema after 7 months of smoke-exposure (Figure 5(A,E,F)).

The immunohistochemical stains for chitinase-3 like protein (ECF-L or Yml) and arginase 1 in the lungs of mice

exposed to cigarette smoke for 5 months are reported in Figures 6 and 7, respectively. These products, that are markers of M2 activation, are differently present in tissue slices from the various strains. In particular, strains that show consistent fibrotic lesions either in subpleural and/or peribronchiolar regions, such as DBA/2 and p66 deficient mice, show a remarkable number of ECF-L (Figure 6(C,D,F)) and arginase 1 positive macrophages (Figure 7(C–F)) in their lungs. A very few numbers of macrophages showing positivity for such products is found in C57 Bl/6 mice (Figures 6(B) and 7(B)), or Lck deficient animals (Figure 6(E)), in which a slight accumulation of collagen can be observed only in the peribronchiolar areas (Figure 2(A,B)). In lungs of ICR mice these marks of M2 activation are not present (Figure 7(A)) or are present in very few pulmonary macrophages (Figure 6(A)).

Of interest, the increase in tissue mRNA expression of ECF-L and arginase 1 (Figure 8(A,B)) parallels the increase in mRNA expression of IL-4, IL-13 and TGF- β (Figure 8(C, D and F), respectively) both in DBA/2 mice and p66 deficient animals. In the latter group, the mRNA expression of iNOS in lung tissue is not significantly different from air control mice of the same strain (Figure 8(E)).

At 5 months, iNOS is highly expressed in lungs of smoking DBA/2, C57Bl/6 and Lck deficient mice. The latter finding offers an explanation for the differences we observed among the various strains of mice in terms of Lm and ISA values (Table 2).

On the other hand, the increase of collagen deposition in smoking DBA/2 (Figure 1(C,D)) and p66shc deficient mice (Figure 2(C,D)) that we observe at 7 months of exposure is preceded by a significant increase of TGF- β expression in their lungs. A slight but significant increase of the expression of this cytokine is also seen in C57 Bl6 and *Lck* knockout mice.

Unlike other groups, no difference in the expression of iNOS, as well as of arginase 1, ECF-L, TGF- β , and other Th2 cytokines, namely IL-4 and IL13, is observed between ICR mice exposed to room air and cigarette smoke.

Discussion

Airflow limitation in COPD is the major feature of the disease that is due to luminal narrowing and progressive obliteration of small airways (*peribronchiolar fibrosis*) and in some individuals to loss of elastic recoil caused by the proteolytic destruction of lung parenchyma (*emphysema*). These mechanisms are not reversible, but their progression may be reduced or prevented by anti-inflammatory or antifibrotic therapies [34].

Inflammation is a driving mechanism in the development and progression of the disease [26]. Neutrophils and macrophages are essential components of inflammation that in concert to other cells of innate immunity (such as eosinophils, mast cells, dendritic cells, NK cells), cells of the adaptive immunity (B and T lymphocytes) and structural cells of the lung (i.e. fibroblasts, endothelial, airway and alveolar epithelial cells) release a lot of inflammatory mediators (enzymes, oxidants and chemokines) that may cause

destructive changes to lung parenchyma and/or remodeling and narrowing processes of small airways [26].

During the early stages of the disease, both neutrophils and macrophages, recruited by the action of cigarette smoke or other irritants, play an essential role in the destructive processes of the lung parenchyma and alveolar attachments of the small airways. However, in the more advanced stages of the disease, macrophages by virtue of their plasticity play a key role in orchestrating the chronic inflammatory response that results in parenchymal and airway remodeling.

Much of knowledge on the pathogenesis of COPD comes from studies done on mouse models obtained by chronic exposure to cigarette smoke. The genetic and physiological similarities to humans and the possibility of creating “tailored models” through genetic manipulation give us the opportunity to study the basis of different disease phenotypes in mice after chronic exposure to cigarette smoke. The large variability of inbred strains is the main cause of different individual responses of mice to cigarette smoke [5].

In this study, we report how the natural plasticity of macrophages may give rise, in different strains of mouse, to multiple phenotypes of disease that are characterized by various cell populations with different functional phenotype and capacity of influencing the inflammatory or reparative responses caused by cigarette smoking.

The activation and the differentiation in M1 and M2 subpopulations can confer to polarized macrophages the capacity to release pro-inflammatory cytokines, nitric oxide (NO) and reactive oxygen intermediates (M1-type response), or secrete a series of substances and anti-inflammatory cytokines that promote proliferation of contiguous cells and tissue repair (M2-type response).

As reported in previous papers, ICR mouse does not develop emphysema and airway changes after chronic exposure to cigarette smoke [6,35,36]. The insensitivity of ICR mouse to the dangerous effects of cigarette smoke has been attributed to high serum alpha1-antitrypsin levels and valid antioxidant defenses due to its strong Nrf2 activity [6,35,36]. This may modify the microenvironment where macrophages reside, thus modifying their natural plasticity and the change in phenotype [37]. Of interest, unlike other strains covered by this study, ICR mice show very few activated macrophages (Mac 3 positive) after chronic exposure to cigarette smoke. These non-polarized cells that are negative to M1 or M2 markers (iNOS or ECF-L and arginase 1, respectively) represent rest macrophages (M0) that can only secrete low levels of pro-inflammatory or anti-inflammatory products.

A large population of M1 positive macrophages is observed in DBA/2, C57 Bl/6 and in Lck deficient mice, which show consistent destructive changes in their lung parenchyma. In these latter strains, M1 cells predominate in the peripheral areas of the lung tissue, where emphysematous lesions are more evident. Pro-inflammatory M1 macrophages release products that damage contiguous tissue and inhibit proliferation of surrounding cells. In particular, they express iNOS, which allows to metabolize arginine into NO, and produce or secrete large quantities of other cytotoxic products such as reactive oxygen intermediates, enzymes

and many other proinflammatory cytokines such as type 1 IFN, IL-6, IL-1, TNF α , CXCL-1-3, -5, -8-10 that can promote proteolysis of extracellular matrix [38] and cytotoxic activity [39]. Various signaling molecules are involved in M1 macrophage polarization [40]. These include transcription factors and inflammatory modulators such as Toll-like receptor (TLR) ligands, recognition receptors such as formyl peptide receptor 1 (FPR1), receptor for advanced glycation end-products (RAGE) or purinergic receptors, or cytokines or chemokines released from injured lung cells. These molecules can play a role in macrophage M1 activation without influence of specialized or polarized T cells (Th1, Th2, Tregs). T cells are severely reduced in Lck ko mice due to the targeted disruption of *Lck* gene that results in severe block in thymocyte maturation [12].

Macrophages can be driven to M2 phenotype by various stimuli such as IL-13, IL-4 and IL-10 [41,42] and hypoxia [43]. The high number of ECF-L and arginase 1 positive macrophages that we observed in our series is probably related to high expression of IL-4 and IL-13 in cigarette smoke sensitive mice. M2 macrophages attenuate inflammation and can promote reparative and remodeling processes with collagen deposition and fibrosis in the surrounded areas through the secretion of TGF- β . This process is favored by the high expression of arginase 1 and ECF-L. In M2 polarized macrophages, IL-4 induces arginase activity, which converts L-arginine to ornithine, a precursor of polyamines and proline, necessary for collagen synthesis from fibroblasts [44], while ECF-L increases collagen production from these cells and stimulates the expression TGF- β [45] and its activation by IL-13 [46].

M2 macrophages are directly involved in the development of intraparenchymal fibroproliferative changes and subpleural fibrosis in DBA/2 mice, and in the peribronchiolar wall remodeling which is observed at 7 months after exposure to cigarette smoke in *p66Shc* knockout mice. These changes are present later on in C57 Bl/6 and Lck deficient mice [12,24]. Of interest, no difference in the expression of ECF-L, arginase 1, IL-4, IL-13 and TGF- β is observed in lungs of DBA/2 and *p66Shc* deficient mice. However, the different compartmentalization of M2 macrophages which we observed in lungs of these mice may explain the difference in the distribution of the fibrotic lesions in strains.

Lung morphology and morphometry (i.e. Lm and ISA) reveal significant difference in terms of emphysematous changes between DBA/2 and *p66Shc* ko mice. This could be explained by the marked difference in the number of macrophages expressing iNOS, which show a M1 pattern of polarization and to the oxidative stress resistance existing between the two strains [47–49]. It is known that *p66Shc* regulates mitochondrial permeability and hence cytochrome C release, by modulating production of oxyradicals (ROS) [50]. ROS production in turn may brought rest macrophages to M1 phenotype, and thus to augment toxic NO in lung microenvironment.

Conclusions

In conclusions, studies carried out in smoking mice from different strains suggest that individual responses in terms

of macrophage activation, polarization and lung compartmentalization can greatly influence chronic inflammatory processes after exposure to cigarette smoke. The difference in the pattern of polarization and distribution in lung can lead to damage and dysfunctional tissue repair, which in some respects are similar to those that can characterize COPD phenotypes in humans.

In addition to the general limitations of the mouse model, such as anatomical or physiological differences [51], the moderate functional and anatomical changes that follow chronic exposure to cigarette smoke in mice can also be a further limiting factor [5]. However, further study in these models is necessary to gain insight into the underlying mechanisms of the disease and to search and develop new compounds with a potential therapeutic activity for COPD patients. New research is now oriented to find molecules capable of regulating macrophage M1-M2 polarization and to target macrophage cytokines [52] and other products, such as YKL-40 (the human counterpart of ECF-L) that in COPD patients is associated with a faster decline of lung function and a high frequency of exacerbations [45,53].

In our opinion, mouse models of COPD involving cigarette smoke should be essential components of this program.

Declaration of interest

The authors report no conflict of interest.

Acknowledgements

All animal experiments were conducted in conformity with the “Guiding Principles for Research Involving Animals and human Beings” and were approved by the Local Ethics Committee of the University of Siena.

Funding

This work was supported by a grant from the Ministero dell’Istruzione, dell’Università e della Ricerca (Rome, Italy) and by a grant from University of Siena (Piano a Sostegno della Ricerca, Siena, Italy).

ORCID

Giovanna De Cunto  <http://orcid.org/0000-0002-3869-4621>
 Eleonora Cavarra  <http://orcid.org/0000-0002-4600-0546>
 Barbara Bartalesi  <http://orcid.org/0000-0002-6792-5249>
 Giuseppe Lungarella  <http://orcid.org/0000-0002-3796-7317>
 Monica Lucattelli  <http://orcid.org/0000-0001-7372-9933>

References

1. Rennard SI, Locantore N, Delafont B, et al. Identification of five chronic obstructive pulmonary disease subgroups with different prognoses in the ECLIPSE cohort using cluster analysis. *Ann Am Thorac Soc*. 2015;12(3):303–312. doi:10.1513/AnnalsATS.201403-125OC.
2. Duffy S, Weir M, Criner GJ. The complex challenge of chronic obstructive pulmonary disease. *Lancet Respir Med*. 2015;3(12):917–919. doi:10.1016/S2213-2600(15)00480-4.

3. Barnes PJ, Burney PG, Silverman EK, et al. Chronic obstructive pulmonary disease. *Nat Rev Dis Primers*. 2015;1:15076. doi:10.1038/nrdp.2015.76.
4. Rahman I, De Cunto G, Sundar IK, et al. Vulnerability and genetic susceptibility to cigarette smoke-induced emphysema in mice. *Am J Respir Cell Mol Biol*. 2017;57(3):270–271. doi:10.1165/rcmb.2017-0175ED.
5. De Cunto G, Cavarra E, Bartalesi B, et al. Innate immunity and cell surface receptors in the pathogenesis of COPD: Insights from mouse smoking models. *COPD*. 2020;15:1143–1154. doi:10.2147/COPD.S246219.
6. Cavarra E, Bartalesi B, Lucattelli M, et al. Effects of cigarette smoke in mice with different levels of alpha(1)-proteinase inhibitor and sensitivity to oxidants. *Am J Respir Crit Care Med*. 2001;164(5):886–890. doi:10.1164/ajrccm.164.5.2010032.
7. Bartalesi B, Cavarra E, Fineschi S, et al. Different lung responses to cigarette smoke in two strains of mice sensitive to oxidants. *Eur Respir J*. 2005;25(1):15–22. doi:10.1183/09031936.04.00067204.
8. Lucattelli M, Bartalesi B, Cavarra E, et al. Is neutrophil elastase the missing link between emphysema and fibrosis? Evidence from two mouse models. *Respir Res*. 2005;6:e83. doi:10.1186/1465-9921-6-83.
9. De Cunto G, Cardini S, Cirino G, et al. Pulmonary hypertension in smoking mice over-expressing protease-activated receptor-2. *Eur Respir J*. 2011;37(4):823–834. doi:10.1183/09031936.00060210.
10. De Cunto G, Brancaleone V, Riemma MA, et al. Functional contribution of sphingosine-1-phosphate to airway pathology in cigarette smoke-exposed mice. *Br J Pharmacol*. 2020;177(2):267–281. doi:10.1111/bph.14861.
11. Lunghi B, De Cunto G, Cavarra E, et al. Smoking p66Shc knocked out mice develop respiratory bronchiolitis with fibrosis but not emphysema. *PLoS One*. 2015;10(3):e0119797. doi:10.1371/journal.pone.0119797.
12. De Cunto G, Lunghi B, Bartalesi B, et al. Severe reduction in number and function of peripheral t cells does not afford protection toward emphysema and bronchial remodeling induced in mice by cigarette smoke. *Am J Pathol*. 2016;186(7):1814–1824. doi:10.1016/j.ajpath.2016.03.002.
13. Cardini S, Dalli J, Fineschi S, et al. Genetic ablation of the Fpr1 gene confers protection from smoking-induced lung emphysema in mice. *Am J Respir Cell Mol Biol*. 2012;47(3):332–333. doi:10.1165/rcmb.2012-0036OC.
14. Cicko S, Lucattelli M, Müller T, et al. Purinergic receptor inhibition prevents the development of smoke-induced lung injury and emphysema. *J Immunol*. 2010;185(1):688–697. doi:10.4049/jimmunol.0904042.
15. Lucattelli M, Cicko S, Müller T, et al. P2X7 receptor signaling in the pathogenesis of smoke-induced lung inflammation and emphysema. *Am J Respir Cell Mol Biol*. 2011;44(3):423–429. doi:10.1165/rcmb.2010-0038OC.
16. Lommatzsch M, Cicko S, Müller T, et al. Extracellular adenosine triphosphate and chronic obstructive pulmonary disease. *Am J Respir Crit Care Med*. 2010;181(9):928–934. doi:10.1164/rccm.200910-1506OC.
17. Fineschi S, De Cunto G, Facchinetti F, et al. Receptor for advanced glycation end products contributes to postnatal pulmonary development and adult lung maintenance program in mice. *Am J Respir Cell Mol Biol*. 2013;48(2):164–171. doi:10.1165/rcmb.2012-0111OC.
18. Stogsdill MP, Stogsdill JA, Bodine BG, et al. Conditional overexpression of receptors for advanced glycation end-products in the adult murine lung causes airspace enlargement and induces inflammation. *Am J Respir Cell Mol Biol*. 2013;49(1):128–134. doi:10.1165/rcmb.2013-0013OC.
19. Robinson AB, Stogsdill JA, Lewis JB, et al. RAGE and tobacco smoke: insights into modeling chronic obstructive pulmonary disease. *Front Physiol*. 2012;3:301. doi:10.3389/fphys.2012.00301.
20. Lazar Z, Müllner N, Lucattelli M, et al. NTPDase1/CD39 and aberrant purinergic signalling in the pathogenesis of COPD. *Eur Respir J*. 2016;47(1):254–263. doi:10.1183/13993003.02144-2014.
21. Atzori L, Lucattelli M, Scotton CJ, et al. Absence of proteinase-activated receptor-1 signaling in mice confers protection from fMLP-induced goblet cell metaplasia. *Am J Respir Cell Mol Biol*. 2009;41(6):680–687. doi:10.1165/rcmb.2007-0386OC.
22. Waseda K, Miyahara N, Taniguchi A, et al. Emphysema requires the receptor for advanced glycation end-products triggering on structural cells. *Am J Respir Cell Mol Biol*. 2015;52(4):482–491. doi:10.1165/rcmb.2014-0027OC.
23. Stockley RA, Grant RA, Llewellyn-Jones CG, et al. Neutrophil formyl-peptide receptors: relationship to peptide-induced responses and emphysema. *Am J Respir Crit Care Med*. 1994;149(2):464–468. doi:10.1164/ajrccm.149.2.8306047.
24. De Cunto G, Bartalesi B, Cavarra E, et al. Ongoing lung inflammation and disease progression in mice after smoking cessation. Beneficial effects of formyl-peptide receptors blockade. *Am J Pathol*. 2018;188(10):2195–2206. doi:10.1016/j.ajpath.2018.06.010.
25. Lungarella G, Cavarra E, Fineschi S, et al. Dual role for proteases in lung inflammation. In: Vergnolle N, Chignard M, editors. *Proteases and their receptors in inflammation*. Basel: Springer; 2011. p. 123–144.
26. Barnes PJ. Cellular and molecular mechanisms of chronic obstructive pulmonary disease. *Clin Chest Med*. 2014;35(1):71–86. doi:10.1016/j.ccm.2013.10.004.
27. Thurlbeck WM. Measurement of pulmonary emphysema. *Am Rev Respir Dis*. 1967;95(5):752–764. doi:10.1164/ajrccm/147.4.975.
28. Saito K, Cagle P, Berend N, et al. Internal surface area of non emphysematous lungs. *Am Rev Respir Dis*. 1989;139(2):308–773. doi:10.1164/ajrccm/139.2.308.
29. Campbell H, Tomkeieff SI. Calculation of the internal surface of a lung. *Nature*. 1952;170(4316):116–117. doi:10.1038/170117a0.
30. Lucattelli M, Fineschi S, Selvi E, et al. Ajulemic acid exerts potent anti-fibrotic effect during the fibrogenic phase of bleomycin lung. *Respir Res*. 2016;17(1):49. doi:10.1186/s12931-016-0373-0.
31. Roviezzo F, Brancaleone V, Mattera Iacono V, et al. Proteinase activated receptor-2 counterbalances the vascular effects of endothelin-1 in fibrotic tight-skin mice. *Br J Pharmacol*. 2017;174(22):4032–4042. doi:10.1111/bph.13618.
32. Weibel ER. Stereological principles for morphometry in electron microscopic cytology. *Int Rev Cytol*. 1969;26:235–302. doi:10.1016/s0074-7696(08)61637-x.
33. Winer J, Jung CK, Shackel I, et al. Development and validation of real-time quantitative reverse transcriptase-polymerase chain reaction for monitoring gene expression in cardiac myocytes in vitro. *Anal Biochem*. 1999;270(1):41–49. doi:10.1006/abio.1999.4085.
34. Hogg JC, Parè PD, Hackett TL. The contribution of the small airway obstruction to the pathogenesis of chronic obstructive pulmonary disease. *Physiol Rev*. 2017;97(2):529–552. doi:10.1152/physrev.00025.2015.
35. Rangasamy T, Misra V, Lee H, et al. Differences in Nrf2 activity between emphysema resistant (ICR) and susceptible (C57Bl/6J) mice strains in response to acute cigarette smoke exposure. *Proc Am Thor Soc*. 2006;3:A129. –
36. Rangasamy T, Cho CY, Thimmulappa RK, et al. Genetic ablation of Nrf2 enhances susceptibility to cigarette smoke-induced emphysema in mice. *J Clin Invest*. 2004;114(9):1248–1259. doi:10.1172/JCI200421146.
37. Mills D, Thomas AC, Lenz LL, et al. Macrophage: SHIP of immunity. *Front Immunol*. 2014;5:620. doi:10.3389/fimmu.2014.00620.
38. Russell RE, Thorley A, Culpitt SV, et al. Alveolar macrophage-mediated elastolysis: roles of matrix metalloproteinases, cysteine, and serine proteases. *Am J Physiol Lung Cell Mol Physiol*. 2002;283(4):L867–L873. doi:10.1152/ajplung.00020.2002.

39. Sica A, Mantovani A. Macrophage plasticity and polarization: in vivo veritas. *J Clin Invest*. 2012;122(3):787–795. doi:10.1172/JCI59643.
40. Wang N, Liang H, Zen Z. Molecular mechanisms that influence the macrophage M1-M2 polarization balance. *Front Immunol*. 2014;5:614. doi:10.3389/fimmu.2014.00614.
41. O'Farrell AM, Liu Y, Moore KW, et al. IL-10 inhibits macrophage activation and proliferation by distinct signaling mechanisms: evidence for Stat3-dependent and -independent pathways. *Embo J*. 1998;17:1006–1018.
42. Lang R, Patel D, Morris JJ, et al. Shaping gene expression in activated and resting primary macrophages by IL-10. *J Immunol*. 2002;169(5):2253–2263. doi:10.4049/jimmunol.169.5.2253.
43. Murdoch C, Lewis CE. Macrophage migration and gene expression in response to tumor hypoxia. *Int J Cancer*. 2005;117(5):701–708. doi:10.1002/ijc.21422.
44. Hesse M, Modolell M, La Flamme AC, et al. Differential regulation of nitric oxide synthase-2 and arginase-1 by type 1/type 2 cytokines in vivo: granulomatous pathology is shaped by the pattern of L-arginine metabolism. *J Immunol*. 2001;167(11):6533–6544. doi:10.4049/jimmunol.167.11.6533.
45. Lai T, Wu D, Chen M, et al. YKL-40 expression in chronic obstructive pulmonary disease: relation to acute exacerbations and airway remodeling. *Respir Res*. 2016;17(1):31. doi:10.1186/s12931-016-0338-3.
46. Kang MJ, Yoon CM, Nam M, et al. Role of chitinase 3-Like-1 in Interleukin-18-induced pulmonary type 1, type 2, and type 17 inflammation; alveolar destruction; and airway fibrosis in the murine lung. *Am J Respir Cell Mol Biol*. 2015;53(6):863–871. doi:10.1165/rcmb.2014-0366OC.
47. Cavarra E, Lucattelli M, Gambelli F, et al. Human SLPI inactivation after cigarette smoke exposure in a new in vivo model of pulmonary oxidative stress. *Am J Physiol Lung Cell Mol Physiol*. 2001;281(2):L412–L417. doi:10.1152/ajplung.2001.281.2.L412.
48. Migliaccio E, Giorgio M, Mele S, et al. The p66shc adaptor protein controls oxidative stress response and life span in mammals. *Nature*. 1999;402(6759):309–313. doi:10.1038/46311.
49. Napoli C, Martin-Padura I, de Nigris F, et al. Deletion of the p66Shc longevity gene reduces systemic and tissue oxidative stress, vascular cell apoptosis, and early atherogenesis in mice fed a high-fat diet. *Proc Natl Acad Sci USA*. 2003;100(4):2112–2116. doi:10.1073/pnas.0336359100.
50. Pellegrini M, Pacini S, Baldari CT. P66SHC: The apoptotic side of SHC proteins. *Apoptosis*. 2005;10(1):13–18. doi:10.1007/s10495-005-6057-8.
51. Martorana PA, Cavarra E, Lucattelli M, et al. Models for COPD involving cigarette smoke. *Drug Discov Today*. 2006;3(3):225–230. doi:10.1016/j.ddmod.2006.09.004.
52. Caramori G, Adcock IM, Di Stefano A, et al. Cytokine inhibition in the treatment of COPD. *Int J Chron Obstruct Pulmon Dis*. 2014;9:397–412. doi:10.2147/COPD.S42544.
53. Guerra S, Halonen M, Sherrill DL, et al. The relation of circulating YKL-40 to levels and decline of lung function in adult life. *Respir Med*. 2013;107(12):1923–1930. doi:10.1016/j.rmed.2013.07.013.